The Impact of Axial Ligation on the Excited State Dynamics of Cobalt(II) Phthalocyanine

Wenhui Hu,^a Denan Wang,^a Qiushi Ma,^a Benjamin J. Reinhart, ^b Xiaoyi Zhang,^{b*} Jier Huang^{a*}

^aDepartment of Chemistry, Marquette University, Milwaukee, Wisconsin, 53201, United States.

^bX-ray Science Division, Argonne National Laboratory, 9700 South Cass Avenue, Argonne, Illinois 60439, United States.

Corresponding Author

Jier Huang (jier.huang@marquette.edu)

Xiaoyi Zhang (xyzhang@anl.gov)

Abstract

In this work, we report the effect of axial ligation on the excited state dynamics of Cobalt phthalocyanines (CoPc) using the combination of X-ray absorption spectroscopy (XAS), transient absorption (TA) spectroscopy, and density functional theory (DFT) calculation. The formation of six coordinated Co center was unambiguously confirmed by XAS when pyridine was used as the solvent, which leads to the prominent blue shift of its Q-band transition with respect to that in weak-ligating solvent (DMF). This is further supported by DFT calculation, which predicted that axial coordination by two pyridine molecules leads to blue shift of Q band. More interestingly, using TA spectroscopy, we observed the formation of a new intermediated state, which is likely due to the further axial ligation of pyridine to CoPc upon photoexcitation, resulting in the quenching of the CoPc excited state and shorter lifetime.

Introduction

Metallophthalocyanines (MPc, Pc=Phthalocyanine) have attracted tremendous interest as an efficient light-harvesting complex to initiate the artificial photosynthesis reaction.[1-4] They also have wide applications in optoelectronics owing to their ultrafast nonlinear optical response arising from their large conjugated π -electron system. [5-8] As the function of MPc for artificial photosynthesis and optoelectronics is largely determined by their light absorption and photophysical properties, it is essential to have fundamental understanding of the excited state (ES) dynamics of MPc. Indeed, The ES dynamics of MPc has been extensively studied using timeresolved absorption spectroscopy supported by quantum mechanical calculations.[9-14] Prior studies have shown that the steady-state absorption and ES dynamics of MPc strongly depend on the central metal of MPc and are sensitive to their host environments.[9, 15-17]. For example, the lifetimes of MPc ES can vary significantly with different transition metal atoms, whereas CoPcs often show a much shorter ES lifetime (~5-10 times shorter) than their Ni and Zn-analogs.[18-20] This was attributed to the coupling of Co orbitals with π -orbitals of the macrocycles of Pc, which provides an additional ES deactivation pathway.[21-23] In addition, axial ligation often occurs in coordinating solvents such as pyridine, imidazole, and pyrazine, which leads to the formation of octahedral geometry from its original square planar structure.[24-31] Depending on the strength of the ligating solvents, the ES relaxation dynamics can take different pathways [32-35] and impact the complex's nucleophilicity and catalytic performance. [36, 37]

While these prior studies provide important insight into the photophysical properties and the ligation mechanism of MPc, the majority of the prior fundamental studies on ES dynamics are based on Ni-MPcs, whereas the investigation of ES dynamics, particularly the impact of ligation on ES dynamics of Co-MPc based are rare.[11, 15, 16, 18, 38] In this work, we report the impact

of pyridine ligation on the ES dynamics of CoPc using the combination of X-ray absorption spectroscopy (XAS), transient absorption (TA) spectroscopy, and density functional theory (DFT) calculation. We show that, in the presence of pyridine, solvent ligation occurs in the ground state. The geometry of CoPc changed from a square planar structure to an octahedral structure in the reaction (Scheme 1), which is unambiguously confirmed by XAS. Upon Q-band excitation, the system quickly relaxes from S₁ to an intermediate state which is associated with a charge transfer (CT) and/or metal-centered (MC) state. Enhanced deactivation of this intermediate state of CoPc is observed in pyridine (ligating solvent) with respect to DMF (weak-ligating solvent). Soret band excitation of CoPc leads to similar relaxation pathways as Q-band excitation except for the initial internal conversion process (S₂-S₁).

Scheme 1. Illustration of axial ligation process in CoPc with pyridine.

Materials

Cobalt Phthalocyanine (CoPc), Dimethylformamide (DMF) and Pyridine were purchased from TCI America. All the chemicals were used as received without further purification.

Characterization.

Steady-state UV-visible absorption spectra were taken using an Agilent 8453 spectrophotometer (UV-Visible) and a Cary 5000 spectrometer.

Time-resolved Absorption (TA) Spectroscopy

The femtosecond TA setup is based on a regenerative amplified Ti-Sapphire laser system (Solstice, 800 nm, <100 fs FWHM, 3.5 mJ/pulse 1 kHz repetition rate). The tunable pump (235-1100 nm), chopped at 500 Hz, is generated in TOPAS (Light Conversion) from 75% of the split output from the Ti-Sapphire laser. The tunable visible probe pulses are generated from the other 25% of the Ti-Sapphire output through white light generation in a Sapphire window (450-750 nm) window on a translation stage. The femtosecond TA measurements are performed in a Helios ultrafast spectrometer (Ultrafast Systems LLC). A 2 mm cuvette with a stir bar inside is used to measure the solution samples, which is kept stirring during the measurement. The TA raw data were processed with background correction as well as time-zero correction. Data analysis was performed with the global analysis using R-package TIMP and Glotaran software, [39, 40] where a three-component model was used to take account of transition: S1 to charge-transfer (CT); CT-solvated-charge-transfer (Ligated-state) and Ligated-state to ground state. Regarding global fitting, IRF parameters (Position = 0.34 and Width = 0.02) and two orders of Dispersion parameters (0.13 and -0.098) were involved and optimized.

Steady state X-ray Absorption Spectroscopy (XAS)

XAS measurement was performed at 12-BM beamline at the Advanced Photon Source (APS), Argonne National Laboratory. The XAS data were collected under room temperature with fluorescence mode using a 13-element germanium solid-state detector. Three ion chambers under the N₂ atmosphere were used and one is placed before the sample for the incident X-ray flux reference signal. The other two ion chambers (second and third chambers) are placed after the sample. The Co foil is placed between the second and third ion chambers and used for energy calibration and collecting Co metal XAS spectrum. The XAS spectra of CoPc in different solvents

were collected using saturated CoPc solutions respectively with five scans in the energy range from 7500 eV to 8500 eV.

UV-visible absorption titration experiment

Concentrated titration (Figure S1a): The 0.05mM of CoPc stock solution is prepared by sonicating the mixture of CoPc (5.715 mg) and 200 mL of anhydrous DMF for 30 mins until the homogeneous solution is obtained. Pure pyridine was directly used as titrant (10uL of titrant is about 0.124 mmol). The titration is conducted with 3 mL of 0.05mM CoPc stock solution followed by adding various amounts of pyridine and the absorption spectra are collected after gently shaking the vial. (Note: the ratio between 10 uL pyridine (0.124 mmol) and 3 mL CoPc stock solution (0.00015 mmol) is about 827).

Diluted titration (Figure S1b):

The diluted pyridine solution in DMF is prepared (60uL/3mL; dilute 50 times) and used as the titrant. The titration was conducted with 3 mL of 0.05mM CoPc stock solution followed by adding various amounts of diluted pyridine solution and the absorption spectra were collected after gently shaking the vial. (Note: the ratio between 10 uL diluted pyridine solution (0.00248 mmol) and 3 mL CoPc stock solution (0.00015 mmol) is about 16.5).

Density Functional Theory (DFT) Calculations.

All DFT calculations were carried out using Gaussian 16 package software[41] installed on the Raj clusters at Marquette University. Geometry optimizations (CoPc, CpPcPy and CoPcPy₂) were carried out using the CAM-B3LYP functional, in combination with the lanl2dz basis set [42-44]. Frequency calculations were carried out to ensure structures represented energetic minima. The TD-DFT calculations were performed based on the optimized structures. The coordinate of optimized structures was listed in the supporting information.

Results and discussion.

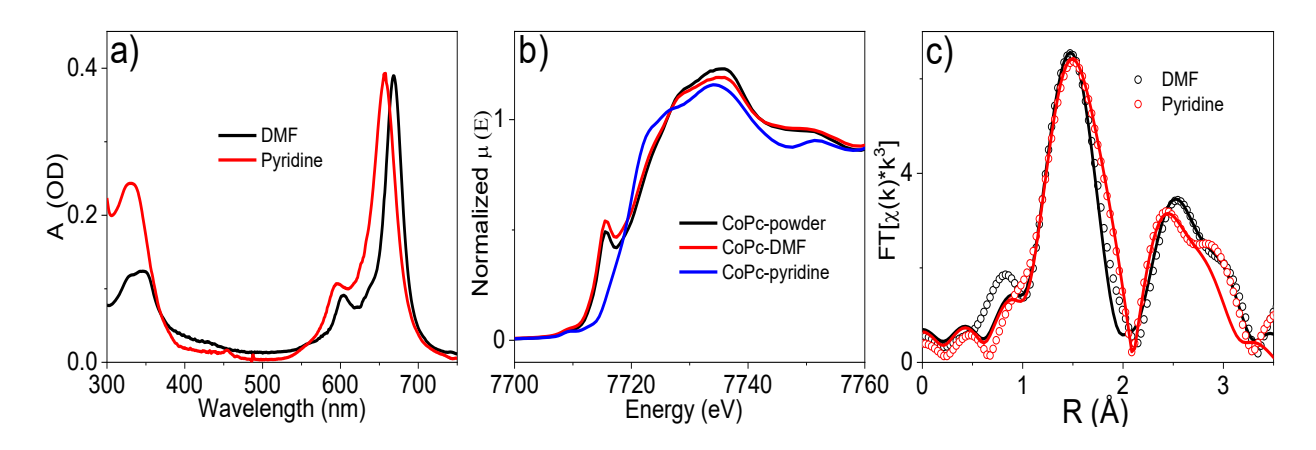


Figure 1. (a) UV-Visible absorption spectra of CoPc (with 0.075 mM concentration) in DMF and pyridine. (b) XANES spectra of CoPc at Co k-edge in DMF, pyridine (2 mg/mL), and solid state. (c) R-space EXAFS spectra of CoPc in DMF and pyridine with K range from 2.5 to 10 Å⁻¹.

The UV-visible absorption spectra of CoPc in DMF (weak-ligating solvent) and pyridine (ligating solvent) are shown in Figure 1a. Two main absorption bands (\sim 350 nm and \sim 650 nm) observed in both solvents, and they can be attributed to the standard Soret band (π - π *) and Q-band (n- π *) of phthalocyanine, respectively.[19] It is interesting to note that the Q-band absorption show prominent blue shift in pyridine with respect to that in DMF. This may be attributed to the change of coordination geometry from square planar to octahedral due to the double axial ligation with solvent pyridine to form CoPcPy and/or CoPcPy₂. As shown in Figure S1, the Q-band transition of CoPc initially shifts to red and then to blue upon the addition of pyridine. Interestingly, Nyokong and co-workers have reported similar titration experiment in DMSO solvent. In contrast, they found that pyridine titration of the pre-formed DMSO-CoPc complex led to red shift of its UV-visible absorption spectrum.[45] The different spectral shift observed between two experiments implies that the formation of solvent-CoPc adducts is likely dependent on the solvent

and may not exist in DMF solvent. However, it is difficult to assign the product only based on the inconspicuous change from UV-Vis titration. The time-dependent density functional theory (TD-DFT) calculation was carried out to get more insight into the information of unligated, monoligated and double-ligated CoPc (Figure S2). Interestingly, the TD-DFT result predicted that the Q-band shifts to red due to the formation of square pyramidal structure in monoaxial ligation (CoPcPy) and shifts to blue due to the formation of CoPcPy₂ with octahedral geometry. These results together suggest that double axial ligation to form CoPcPy₂ dominates in the system with pure pyridine.

X-ray absorption spectroscopy (XAS), a powerful technique that can provide electronic structure and chemical states of materials in both solid and solution phases, is expected to provide valuable information of the ligation process, including the impact of ligation on the change of Co coordination geometry and Co-N bond length. As a result, steady-state XAS was used to examine the local coordination geometry of CoPc at Co center in both DMF and pyridine. The XAS of the powder sample of CoPc was also collected to understand the impact of solvent on the coordination geometry. As shown in Figure 1b, the Co k-edge X-ray near-edge absorption structure (XANES) spectrum of CoPc in solid-state shows two distinct dipole-allowed transition features in the rising

Table 1. Fitting parameters of EXAFS spectra for CoPc in solid state, DMF, and pyridine.

CoPc	Vector	N	$\sigma^2(Å^2)$	R (Å)
Solid state	Co-N ₁	4	0.003	1.92
	Co-C	8	0.004	2.96
	Co-N ₂	4	0.003	3.25
DMF	Co-N ₁	4	0.005	1.92
	Co-C	8	0.005	2.96
	Co-N ₂	4	0.002	3.26
Pyridine	Co-N ₁	4	0.005	1.92
	Co-C	8	0.006	2.94
	Co-N ₂	4	0.004	3.25
	Co-N ₃	2	0.006	2.31

edge: a sharp peak at 7715 eV corresponding to 1s to 4pz transition and a white line transition at \sim 7735 eV corresponding to 1s to 4p_{x,y} transition. There is also a weak, 1s-3d pre-edge transition feature at about 7709 eV due to the mixing of 3d-4p orbitals. Such mixing is only allowed in a non-centrosymmetric system. These spectral features are similar to that of previously reported CoPc and Co porphyrins, [46-49] suggesting that CoPc adopts square planar geometry in solidstate. Note that similar spectral features are observed in the XANES spectrum of CoPc in DMF, suggesting that square planar structure retains in DMF and the presence of DMF has a negligible impact on the coordination geometry of Co center, i.e. DMF is a weak-ligating solvent. In contrast, the peak corresponding to 1s-4pz transition in the XANES spectrum of CoPc in pyridine disappears, suggesting the change of Co coordination environment due to solvent ligation. This solvent ligation reduces the degeneracy among 4p orbitals where 1s-4pz transition energy shifts up and becomes indistinguishable from 1s to 4p_{x,y} transition. To further understand how the local structure of Co center changes in pyridine with respect to weak-ligating solvent DMF, we quantitatively analyzed the extended X-ray absorption fine structure (EXAFS) spectra in both solvents (Figure S3). The EXAFS spectra of CoPc in DMF and solid-state can be adequately fit by the proposed square planar model which was built and optimized by DFT calculation, where similar first shell Co-N₁ (1.92 Å, N=4), and second shell Co-C (2.96 Å, N=8) and Co-N₂ (3.25(6) Å, N=4) bond distances are obtained. However, significant deviations were observed when the same square planar model was used to fit the EXAFS spectrum of CoPc in pyridine. Instead, the EXAFS spectrum of CoPc in pyridine can be well fit with an octahedral model, where an additional Co-N₃ path (2.31 Å, N=2) is used to take account of the axial ligation of pyridine to Co center in CoPc as illustrated in Scheme 1. This assignment is further supported by the Fourier transformed

EXAFS spectrum in R space, where broader first shell peak was observed for CoPc in pyridine (Figure 1c) due to the presence of additional Co-N₃ paths from pyridine ligation.

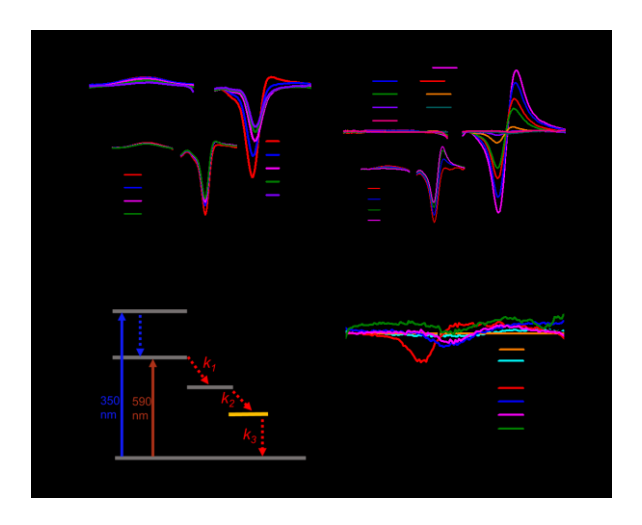


Figure 2. Femtosecond TA spectra of CoPc (with 0.075 mM concentration) in DMF (a) and pyridine (c) under 590 nm excitation. (b) Energetics diagram that illustrates the excited state relaxation dynamics of CoPc. (d) The zoom-in TA spectra of CoPc in pyridine at 500-700 nm region after 40 ps.

To shed light on the impact of ligation on the photophysical properties of CoPc, we examined its ES dynamics in DMF and pyridine using transient absorption (TA) spectroscopy. Figure 2a shows the TA spectra of CoPc in DMF following the excitation of Q band (S_0 - S_1) at 590 nm (Figure 2b). Immediately following the excitation, the TA spectra of CoPc show a negative feature at \sim 660 nm and a broad absorption centered at 510 nm which can be attributed to the ground state bleach (GSB) and the excited state (E1, S_1 - S_n) absorption, respectively. There is also a negative feature at \sim 705 nm which comes from the solvent Raman scattering. The solvent Raman scattering quickly disappears (< 0.4 fs), after which the growth of a new absorption (\sim 690 nm, E2) is observed within 1 ps. Because the formation of E2 is accompanied by the decay of E1 and recovery of GSB, E2 can be attributed to a new intermediate species that is distinct from E1. According to

previous studies on transition metal Pc complexes, E2 is likely due to the formation of a charge-transfer (CT) state or metal-centered (MC) state.[50] After E2 is fully developed, both E1 and E2 decay simultaneously with the recovery of GSB, which is featured by two isosbestic points at 568 nm and 677 nm, respectively, suggesting that these spectral evolutions represent the same relaxation process, i.e. E1 and E2 return to ground state.

Compared to the TA spectra in DMF, the spectra in pyridine show distinct spectral features. As shown in the inset of Figure 2c, although the early time spectra exhibit the E1, GSB, stimulated emission (< 0.4 ps), and the formation of E2 (> 0.4 ps), the decay of E1 and the formation of E2 are more prominent. This can be more clearly seen in the later time spectra (Figure 2c), where the amplitude of E2 is much more intense than that in the TA spectra of CoPc in DMF (Figure 2a). After that, E1 and E2 decay simultaneously with the recovery of GSB, as evidenced by the isosbestic points at 548 nm and 665 nm, respectively, suggesting the system returns to ground state from E1 and E2. However, a careful inspection of the later time spectra (> 70 ps) shows an additional spectral evolution with the formation of a positive signal at ~ 650 nm and a negative signal at ~ 675 nm, which together forms a derivative feature (Figure 2d) which is absent in DMF (Figure S5). Since this new feature bleaches out the red shoulder of the CoPc ground state, it is likely associated with an additional intermediate state with blue-shifted Q band absorption. Although the nature of this state remains unclear, it might be a state related to the ligation of pyridine upon photoexcitation, which is supported by the previously reported work, where the similar spectral features were observed in a NiPc complex.[36] This can occur because it is possible that a small fraction of CoPc may not be fully ligated in the ground state, allowing additional ligation in the excited state.

To examine the impact of the excitation wavelength on the ES dynamics, we collected the TA spectra of CoPc in DMF and pyridine under 350 nm excitation which excites the Soret band (S₀-S₂) of Pc molecule. Similar to the TA spectra with Q-band (590 nm) excitation, the TA spectra with Soret band excitation (350 nm) are featured by E1, E2, and GSB at same wavelengths as that of Q-band transition (Figure S4). Instead of decay of E1 and recovery of GSB at < 1ps upon Q-band excitation, E1 and GSB grow with time upon Soret band excitation. After that, the TA spectra at later time show similar spectral evolutions as that of Q-band excitation. These results together suggest that the early time rising component for E1 and GSB arises from the internal conversion from S₂-S₁ (Figure 2b), after which the system follows the same relaxation pathway as that of Q-band excitation.

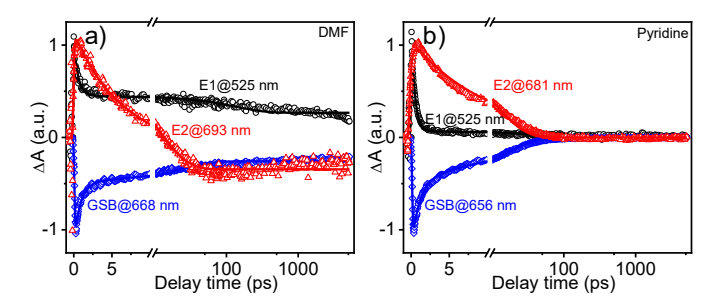


Figure 3. The kinetic traces of E1, E2 and GSB of TA spectra of CoPc in DMF (a) and pyridine (b) under 590 nm excitation.

To quantitatively evaluate the impact of ligation on the ES relaxation dynamics of CoPc, we compared the kinetics traces at E1, E2 and GSB in DMF and pyridine. As shown in Figure 3a, the early time kinetics of E1 (525 nm) for CoPc in DMF decays immediately following 590 nm excitation whereas the kinetics of E2 (693 nm) has an obvious rising component that can be attributed to the formation of E2 due to relaxation from S_1 to CT/MC (k_I , Figure 2b), consistent with early time spectral evolution discussed above. The similar decay/rising time were also observed in E1/E2 kinetics in pyridine (Figure 3b) but the average lifetimes for these features are

significantly different. The E1, E2, and GSB in DMF all have a long-lived component (Figure 3a), which is much longer than our TA time window (5 ns). However, the lifetimes of these species in pyridine are less than 100 ps, the kinetics results of CoPc in DMF and pyridine solvent showed similar trend compared to the reported NiPc in the coordinated and uncoordinated solvents, the much shorter excited state lifetime in coordinated solvents. Compared to NiPc, the excited state lifetime of CoPc (< 100 ps) in pyridine in this work is much smaller, which may be due to the intrinsic difference between Co and Ni and the functional group in NiPc. These kinetic traces can be well fitted by global target analysis (Figure S6 and S7), where a three-component model was used to take account of k_1 , k_2 , and k_3 (Figure 2b). Note that the fourth component was not necessary to account for the direct relaxation from S_1 to ground state (k_0), suggesting that S_1 to CT/MC is the dominating pathway for S₁ relaxation. As can be seen from the global analysis results, the ligation slightly impacts k_1 and k_2 , which leads to $\tau_1 = 0.3$ ps and $\tau_2 = 11$ ps in DMF, and $\tau_1 = 0.6$ ps and $\tau_2 = 10$ ps in pyridine, respectively. However, significant change is observed for k_3 , for which the lifetime reduces from 12 ns to 79 ps when the solvent changes from DMF to pyridine. This is consistent with our assignment above, where the ligation of pyridine in excited state occurs at later time of the TA spectra and results into the quenching of k_3 .

Conclusion.

In summary, we investigated the axial ligation effect using pyridine as the ligating solvent on CoPc molecule while DMF was used as the reference weak-ligating solvent. The steady-state X-ray absorption spectroscopy results showed the local geometry of Co center changes in pyridine (octahedral geometry) compared to that in DMF and solid state (square planar). The changes to the octahedral geometry lead to the blue shift of Q-band in the UV-visible absorption spectra, which is consistent with TD-DFT prediction. The TA spectra showed the formation of an

additional intermediate state in pyridine, which can be attributed to the formation of the ligated state due to photoexcitation of CoPc. Overall, our studies support that the pyridine axial ligation can affect the ground state electronic structure and excited state relaxation dynamics of CoPc.

Conflicts of interest.

There are no conflicts to declare

Author Contributions

The manuscript was written through contributions of all authors. All authors have given approval to the final version of the manuscript.

Acknowledgements

This work was supported by National Science Foundation (DMR-1654140). Use of the Advanced Photon Source in Argonne National Laboratory was supported by the U. S. Department of Energy, Office of Science, Office of Basic Energy Sciences, under Award No. DE-AC02-06CH11357.

Reference

- [1] C.G. Claessens, U. Hahn, T. Torres, Phthalocyanines: From outstanding electronic properties to emerging applications, Chemical Record, 8 (2008) 75-97.
- [2] K. Kasuga, M. Tsutsui, Some new developments in the chemistry of metallophthalocyanines, Coordin Chem Rev, 32 (1980) 67-95.
- [3] S. Fukuzumi, T. Honda, T. Kojima, Structures and photoinduced electron transfer of protonated complexes of porphyrins and metallophthalocyanines, Coordin Chem Rev, 256 (2012) 2488-2502. [4] J.J. Guo, S.R. Wang, X.G. Li, M.Y. Yuan, The synthesis, photophysical and thermal properties of novel 7-hydroxy-4-methylcoumarin tetrasubstituted metallophthalocyanines with axial chloride ligand, Dyes and Pigments, 93 (2012) 1463-1470.
- [5] M. Hanack, T. Schneider, M. Barthel, J.S. Shirk, S.R. Flom, R.G.S. Pong, Indium phthalocyanines and naphthalocyanines for optical limiting, Coordin Chem Rev, 219 (2001) 235-258.

- [6] E.S. Manas, F.C. Spano, L.X. Chen, Nonlinear optical response of cofacial phthalocyanine dimers and trimers, J Chem Phys, 107 (1997) 707-719.
- [7] F.Z. Henari, Optical switching in organometallic phthalocyanine, Journal of Optics a-Pure and Applied Optics, 3 (2001) 188-190.
- [8] P. Wang, S.A. Zhang, P.J. Wu, C. Ye, H.W. Liu, F. Xi, Optical limiting properties of optically active phthalocyanine derivatives, Chem Phys Lett, 340 (2001) 261-266.
- [9] J.Y. Hong, M.S. Kelley, M.L. Shelby, D.K. Hayes, R.G. Hadt, D. Rimmerman, X.Y. Zhang, L.X. Chen, The Nature of the Long-Lived Excited State in a Ni-II Phthalocyanine Complex Investigated by X-Ray Transient Absorption Spectroscopy, Chemsuschem, 11 (2018) 2421-2428.
- [10] L.X. Chen, G.B. Shaw, D.M. Tiede, X.B. Zuo, P. Zapol, P.C. Redfern, L.A. Curtiss, T. Sooksimuang, B.K. Mandal, Excited state dynamics and structures of functionalized phthalocyanines. 1. Self-regulated assembly of zinc helicenocyanine, J Phys Chem B, 109 (2005) 16598-16609.
- [11] G.R. Loppnow, D. Melamed, A.R. Leheny, A.D. Hamilton, T.G. Spiro, Excited-state photophysics of donor-appended cobalt(II) porphyrins from picosecond transient absorption spectroscopy, J Phys Chem-Us, 97 (1993) 8969-8975.
- [12] B.W. Caplins, T.K. Mullenbach, R.J. Holmes, D.A. Blank, Femtosecond to nanosecond excited state dynamics of vapor deposited copper phthalocyanine thin films, Phys Chem Chem Phys, 18 (2016) 11454-11459.
- [13] G. Ricciardi, A. Rosa, E.J. Baerends, Ground and excited states of zinc phthalocyanine studied by density functional methods, J Phys Chem A, 105 (2001) 5242-5254.
- [14] K.M. Murali, S. Baskaran, M.N. Arumugham, Photochemical and DFT/TD-DFT study of trifluoroethoxy substituted asymmetric metal-free and copper(II) phthalocyanines, Journal of Fluorine Chemistry, 202 (2017) 1-8.
- [15] A. Gadalla, O. Cregut, M. Gallart, B. Honerlage, J.B. Beaufrand, M. Bowen, S. Boukari, E. Beaurepaire, P. Gilliot, Ultrafast Optical Dynamics of Metal-Free and Cobalt Phthalocyanine Thin Films, J Phys Chem C, 114 (2010) 4086-4092.
- [16] A. Gadalla, J.B. Beaufrand, M. Bowen, S. Boukari, E. Beaurepaire, O. Cregut, M. Gallart, B. Honerlage, P. Gilliot, Ultrafast Optical Dynamics of Metal-Free and Cobalt Phthalocyanine Thin Films II: Study of Excited-State Dynamics, J Phys Chem C, 114 (2010) 17854-17863.
- [17] D. Kim, D. Holten, M. Gouterman, Evidence from picosecond transient absorption and kinetic studies of charge-transfer states in copper (II) porphyrins, J Am Chem Soc, 106 (1984) 2793-2798. [18] Y.L. Yan, S. Lu, B. Li, R.Y. Zhu, J.H. Zhou, S.H. Wei, S.X. Qian, Ultrafast excited state dynamics of modified phthalocyanines: p-HPcZn and p-HPcCo, J Phys Chem A, 110 (2006)
- [19] L. Howe, J.Z. Zhang, Ultrafast studies of excited-state dynamics of phthalocyanine and zinc phthalocyanine tetrasulfonate in solution, J Phys Chem A, 101 (1997) 3207-3213.

10757-10762.

- [20] L. Howe, J.Z. Zhang, The effect of biological substrates on the ultrafast excited-state dynamics of zinc phthalocyanine tetrasulfonate in solution, Photochem Photobiol, 67 (1998) 90-96.
- [21] A.V. Nikolaitchik, M.A.J. Rodgers, Crown ether substituted monomeric and cofacial dimeric metallophthalocyanines. 2. Photophysical studies of the cobalt(II) and nickel(II) variants, J Phys Chem A, 103 (1999) 7597-7605.
- [22] M.-S. Liao, S. Scheiner, Electronic structure and bonding in metal phthalocyanines, metal= Fe, Co, Ni, Cu, Zn, Mg, The Journal of Chemical Physics, 114 (2001) 9780-9791.

- [23] P.S. Vincett, E.M. Voigt, Rieckhof.Ke, Phosphorescence and Fluorescence of Phthalocyanines, J Chem Phys, 55 (1971) 4131-4140.
- [24] J. Janczak, R. Kubiak, Stereochemistry and properties of the M(II)-N(py) coordination bond in the low-spin dipyridinated iron(II) and cobalt(II) phthalocyanines, Inorg Chim Acta, 342 (2003) 64-76.
- [25] M.S. Liao, J.D. Watts, M.J. Huang, DFT study of unligated and ligated manganese(II) porphyrins and phthalocyanines, Inorg Chem, 44 (2005) 1941-1949.
- [26] D.E. Yu, A. Kikuchi, T. Taketsugu, T. Inabe, Crystal Structure of Ruthenium Phthalocyanine with Diaxial Monoatomic Ligand: Bis(Triphenylphosphine) Iminium Dichloro(Phthalocyaninato(2-)) Ruthenium(III), Journal of Chemistry, 2013 (2013).
- [27] A.B.P. Lever, J.P. Wilshire, Redox potentials of metal phthalocyanines in non-aqueous media, Can J Chem, 54 (1976) 2514-2516.
- [28] G. Kwag, E. Park, S. Kim, Self-assembled and alternative porphyrin-phthalocyanine array, B Kor Chem Soc, 25 (2004) 298-300.
- [29] X.B. Leng, C.F. Choi, P.C. Lo, D.K.P. Ng, Assembling a mixed phthalocyanine-porphyrin array in aqueous media through host-guest interactions, Org Lett, 9 (2007) 231-234.
- [30] F. Cariati, D. Galizzioli, F. Morazzoni, C. Busetto, New adducts of phthalocyaninatocobalt (II) with pyridine and 4-methylpyridine and their vibrational, magnetic, and electronic properties. Part I. Reactivity towards oxygen, Journal of the Chemical Society, Dalton Transactions, (1975) 556-561.
- [31] J.M. Assour, Solvent effects on the spin resonance spectra of cobalt phthalocyanine, J Am Chem Soc, 87 (1965) 4701-4706.
- [32] J. Rodriguez, D. Holten, Ultrafast vibrational dynamics of a photoexcited metalloporphyrin, J Chem Phys, 91 (1989) 3525-3531.
- [33] J. Rodriguez, D. Holten, Ultrafast photodissociation of a metalloporphyrin in the condensed phase, J Chem Phys, 92 (1990) 5944-5950.
- [34] J. Rodriguez, C. Kirmaier, D. Holten, Time-resolved and static optical-properties of vibrationally excited porphyrins, J Chem Phys, 94 (1991) 6020-6029.
- [35] L.X. Chen, X.Y. Zhang, E.C. Wasinger, J.V. Lockard, A.B. Stickrath, M.W. Mara, K. Attenkofer, G. Jennings, G. Smolentsev, A. Soldatov, X-ray snapshots for metalloporphyrin axial ligation, Chem Sci, 1 (2010) 642-650.
- [36] J.Y. Hong, T.J. Fauvell, W. Helweh, X.Y. Zhang, L.X. Chen, Investigation of the photoinduced axial ligation process in the excited state of nickel(II) phthalocyanine, J Photoch Photobio A, 372 (2019) 270-278.
- [37] K.E. Rivera Cruz, Y. Liu, T.L. Soucy, P.M. Zimmerman, C.C. McCrory, Increasing the CO2 Reduction Activity of Cobalt Phthalocyanine by Modulating the σ-donor Strength of Axially Coordinating Ligands, Acs Catal, 11 (2021) 13203-13216.
- [38] Z.G. Li, C.Y. He, J.Z. Fan, Y.Q. Wu, Y.S. Liu, J.F. Feng, Y.L. Song, Optical nonlinearities and excited state dynamics of self-assembled cobalt phthalocyanine multilayer films, Mater Lett, 221 (2018) 279-281.
- [39] I.H.M. van Stokkum, D.S. Larsen, R. van Grondelle, Global and target analysis of time-resolved spectra (vol 1658, pg 82, 2004), Bba-Bioenergetics, 1658 (2004) 262-262.
- [40] J.J. Snellenburg, S.P. Laptenok, R. Seger, K.M. Mullen, I.H.M. van Stokkum, Glotaran: A Java-Based Graphical User Interface for the R Package TIMP, J Stat Softw, 49 (2012) 1-22.
- [41] M.J. Frisch, G.W. Trucks, H.B. Schlegel, G.E. Scuseria, M.A. Robb, J.R. Cheeseman, G. Scalmani, V. Barone, G.A. Petersson, H. Nakatsuji, X. Li, M. Caricato, A.V. Marenich, J. Bloino,

- B.G. Janesko, R. Gomperts, B. Mennucci, H.P. Hratchian, J.V. Ortiz, A.F. Izmaylov, J.L. Sonnenberg, Williams, F. Ding, F. Lipparini, F. Egidi, J. Goings, B. Peng, A. Petrone, T. Henderson, D. Ranasinghe, V.G. Zakrzewski, J. Gao, N. Rega, G. Zheng, W. Liang, M. Hada, M. Ehara, K. Toyota, R. Fukuda, J. Hasegawa, M. Ishida, T. Nakajima, Y. Honda, O. Kitao, H. Nakai, T. Vreven, K. Throssell, J.A. Montgomery Jr., J.E. Peralta, F. Ogliaro, M.J. Bearpark, J.J. Heyd, E.N. Brothers, K.N. Kudin, V.N. Staroverov, T.A. Keith, R. Kobayashi, J. Normand, K. Raghavachari, A.P. Rendell, J.C. Burant, S.S. Iyengar, J. Tomasi, M. Cossi, J.M. Millam, M. Klene, C. Adamo, R. Cammi, J.W. Ochterski, R.L. Martin, K. Morokuma, O. Farkas, J.B. Foresman, D.J. Fox, Gaussian 16 Rev. C.01, in, Wallingford, CT, 2016.
- [42] C. Latouche, D. Skouteris, F. Palazzetti, V. Barone, TD-DFT Benchmark on Inorganic Pt(II) and Ir(III) Complexes, J Chem Theory Comput, 11 (2015) 3281-3289.
- [43] T. Yanai, D.P. Tew, N.C. Handy, A new hybrid exchange-correlation functional using the Coulomb-attenuating method (CAM-B3LYP), Chem Phys Lett, 393 (2004) 51-57.
- [44] L. Ji, A. Lorbach, R.M. Edkins, T.B. Marder, Synthesis and Photophysics of a 2,7-Disubstituted Donor–Acceptor Pyrene Derivative: An Example of the Application of Sequential Ir-Catalyzed C–H Borylation and Substitution Chemistry, The Journal of Organic Chemistry, 80 (2015) 5658-5665.
- [45] T. Nyokong, Equilibrium and kinetic studies of the reaction between pyridine and cobalt (II) phthalocyanine in DMSO, Polyhedron, 14 (1995) 2325-2329.
- [46] N. Lahanas, P. Kucheryavy, J.V. Lockard, Spectroscopic Evidence for Room Temperature Interaction of Molecular Oxygen with Cobalt Porphyrin Linker Sites within a Metal-Organic Framework, Inorg Chem, 55 (2016) 10110-10113.
- [47] Z.J. Yang, X.F. Zhang, C. Long, S.H. Yan, Y.N. Shi, J.Y. Han, J. Zhang, P.F. An, L. Chang, Z.Y. Tang, Covalently anchoring cobalt phthalocyanine on zeolitic imidazolate frameworks for efficient carbon dioxide electroreduction, Crystengcomm, 22 (2020) 1619-1624.
- [48] I. Yamanaka, R. Ichihashi, T. Iwasaki, N. Nishimura, T. Murayama, W. Ueda, S. Takenaka, Electrocatalysis of heat-treated cobalt-porphyrin/carbon for hydrogen peroxide formation, Electrochim Acta, 108 (2013) 321-329.
- [49] Y.S. Liu, A. Deb, K.Y. Leung, W.X. Nie, W.S. Dean, J.E. Penner-Hahn, C.C.L. McCrory, Determining the coordination environment and electronic structure of polymer-encapsulated cobalt phthalocyanine under electrocatalytic CO2 reduction conditions using in situ X-Ray absorption spectroscopy, Dalton T, 49 (2020) 16329-16339.
- [50] T.C. Gunaratne, A.V. Gusev, X.Z. Peng, A. Rosa, G. Ricciardi, E.J. Baerends, C. Rizzoli, M.E. Kenney, M.A.J. Rodgers, Photophysics of octabutoxy phthalocyaninato-Ni(II) in toluene: Ultrafast experiments and DFT/TDDFT studies, J Phys Chem A, 109 (2005) 2078-2089.

TOC

